Supporting information

Elimination of Uremic Toxins by Functionalized Graphene-based Composite Beads for Direct Hemoperfusion

Abhishek Tyagi,[†‡] Yik Wong Ng,[‡] Mohsen Tamtaji,[‡] Irfan Haider Abidi,[‡] Jingwei Li,[‡] Faisal Rehman,[‡] Md Delowar Hossain,[‡] Yuting Cai,[‡] Zhenjing Liu,[‡] Patrick Ryan Galligan,[‡] Shaojuan Luo,[‡§] Kai Zhang,[*†] Zhengtang Luo[*‡]

[†]*State Key Laboratory of Precision Electronic Manufacturing Technology and Equipment, School of Electromechanical Engineering, Guangdong University of Technology, Guangzhou 510006, China.*

[‡]*Department of Chemical and Biological Engineering, William Mong Institute of Nano Science and Technology, and Hong Kong Branch of Chinese National Engineering Research Center for Tissue Restoration and Reconstruction, the Hong Kong University of Science and Technology, Clear Water Bay, Kowloon, Hong Kong.*

[§]*School of Chemical Engineering and Light Industry, Guangdong University of Technology, Guangzhou 510006, China.*

[*] *Corresponding author email: zhangkai@gdut.edu.cn, keztluo@ust.hk.*

Table of content

1. Experimental setup

a. For *in vivo* blood perfusion: The protocol was adopted from the previously published research.[1-2] Chemicals and animal treatment: All the rats (n=30) were anesthetized by 3.5% chloral hydrate at intraperitoneal injection (1 mL 100^{-1} g of body weight). Other chemicals that were used are buprenorphine for post-operative analgesia, sterile alcohol prep pads, sterile heparin sodium injection, sterile saline solution saline, and isopropyl alcohol 70%, polyethylene catheters.

Surgical equipment's: Scissors, forceps and needle holders, sterilized hemoadsorption cartridge, rotary mini-pump, heating pad, clinical thermometers. Gauge bendable tips, gauge & gauge needles.

Procedures: The experiments were complied with law and regulations for research use policy of animals, the procedure was adopted by previously published research.[1] Surgical areas were shaved by trimmer and cleaned by 70% Isopropyl alcohol. Animal were placed on their back, and their head were arranged opposite to the operator on the Styrofoam pad, tubes and equipment's were sterilized with 70% isopropyl alcohol, and tubes were passed with heparin 30 IU mL^{-1} saline. Animal was disinfected by iodophor, and dissection of femoral vein was done by microdissection scissors. Then, 18g intravenous indwelling catheters were placed into the femoral artery and femoral vein. All tubing was previously filled with 0.1% sodium heparin-physiological saline solution, and pump flow rate was set for 12 mL min^{-1}. All experiments were conducted at the pH ~7.8, and temperature of 36–37 °C, and temperature was maintained by using heating pad. 100 μL of a 2.5 mg 100 g^{-1} body weight heparin sodium solution was injected along the intravenous indwelling catheter. Extracorporeal circulation stabilized for 10 min. The tenth minute was taken as the first sampling point, and the sample was taken every 5 min, and 500 μL of blood was taken each time, for a total of five samples.

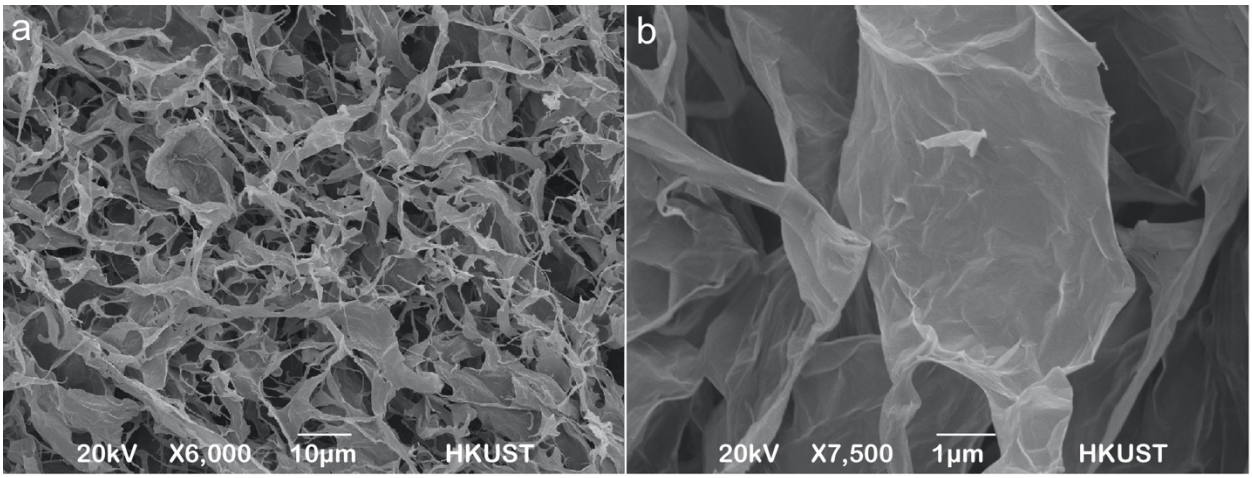

Figure S1: SEM image of graphene oxide. (a) at 10 µm and (b) at 1 µm.

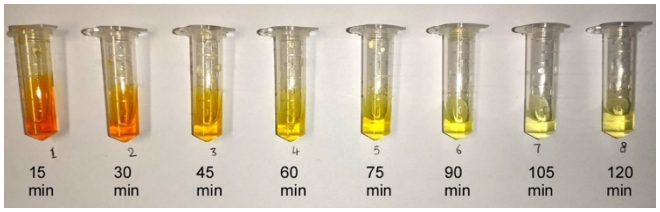

Figure S2: Adsorption for graphene-based adsorbents for bilirubin. The depletion of bilirubin colour was observed with respect to the time of adsorption, the experiment was performed for 120 minutes, and the data was collected after the interval of 15 minutes. The concentration is determined from the UV-Vis spectra using the absorbance at 438 nm for bilirubin adsorption.

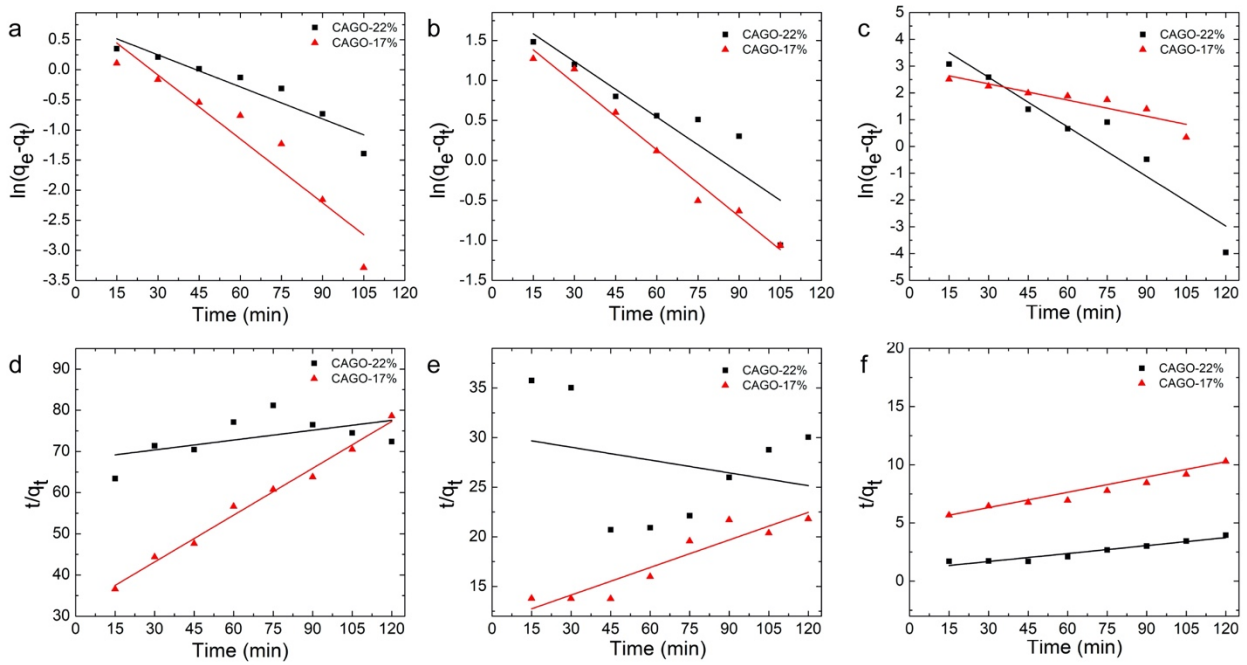

Figure S3: Adsorption kinetics for creatinine, uric acid and bilirubin. Pseudo first order kinetic model for (a) creatinine, (b) uric acid, (c) bilirubin. Pseudo second order kinetic model for (d) creatinine, (e) uric acid, (f) bilirubin. All the calculations were performed on CAGO-22% and CAGO-17% beads and all the experiments were repeated three times.

Sample	Creatinine				Uric acid				Bilirubin			
	Q_e	k_1	q_e	R^2	Q_e	k_1	q_e	R^2	Q_e	k_1	q_e	R^2
CAGO-22%	1.65	0.01	1.62	0.95	3.99	0.022	3.87	0.97	30.43	0.04	30.49	0.94
CAGO-17%	1.52	0.02	1.35	0.95	5.50	0.02	5.57	0.94	11.61	0.01	11.39	0.88

Table S1: Pseudo-first-order kinetic model parameters of creatinine, uric acid, and bilirubin for CAGO-22% and CAGO-17%.

Sample	Creatinine			Uric acid			Bilirubin		
	k_2	R^2	q_e	k_2	R^2	q_e	k_2	R^2	q_e
CAGO-22%	2.31	0.30	12.53	17.75	0.069	23.20	1911.43	0.93	43.85
CAGO-17%	0.21	0.98	2.63	10.28	0.87	10.79	91.82	0.42	-35.08

Table S2: Pseudo-second-order kinetic model parameters of creatinine, uric acid, and bilirubin for CAGO-22% and CAGO-17%.

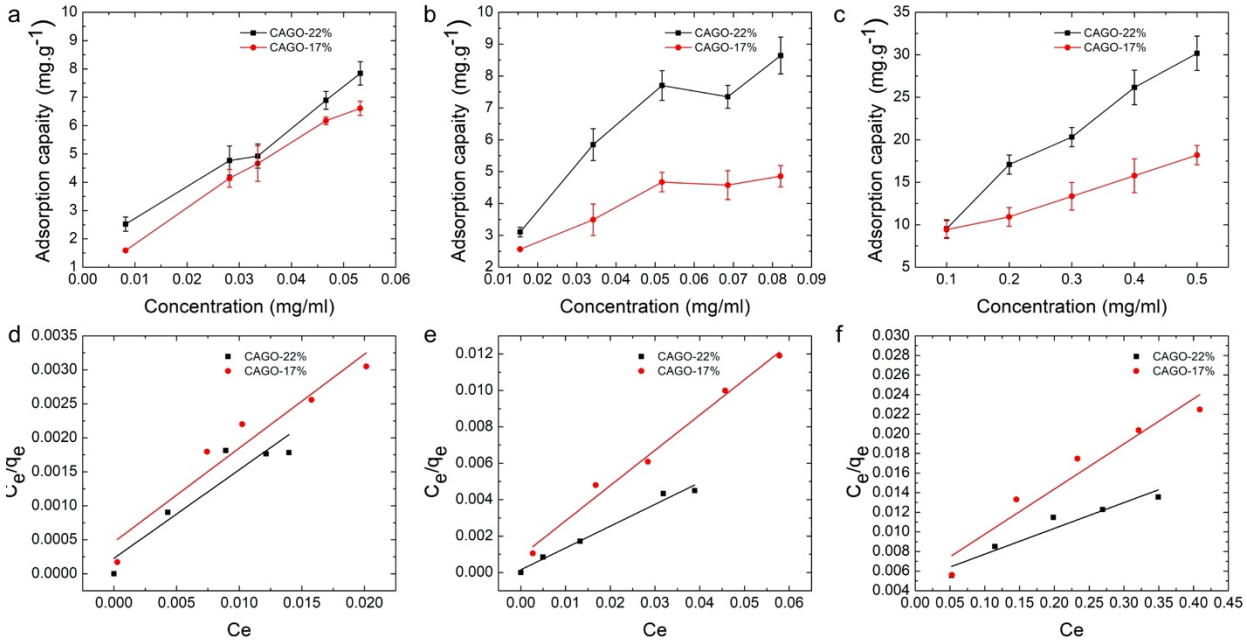

Figure S4: Adsorption and Langmuir isotherm. The adsorption isotherm for (a) creatinine, (b) uric acid, and (c) bilirubin. Langmuir isotherms was estimated at different concentrations for (d) creatinine, (e) uric acid, and (f) bilirubin. All the experiment was performed three times, and all the UV adsorption was recorded.

Sample	Creatinine			Uric acid			Bilirubin		
	K_L	q_{max}	R^2	K_L	q_{max}	R^2	K_L	q_{max}	R^2
CAGO-22%	276.4	7.23	0.92	215.44	5.15	0.98	9.03	21.69	0.93
CAGO-17%	651.5	7.67	0.87	1199	8.34	0.92	5.156	38.02	0.95

Table S3: Langmuir isotherm parameters for creatinine, uric acid, and bilirubin adsorption on CAGO-22% and CAGO-17%.

2. Supplementary Note 1:

a. Blood flow rate and blood loss test:

For blood flow rate as shown in Figure S5b, the blood was drawn from a blood tank (200 mL beaker) driven by a rotatory liquid pump and sent to the cartridge packed with adsorbent and further collected in a measuring cylinder (10 mL). The flow rate of pump was 10.01 mL min^{-1} for these tests, and the blood was collected within a period of 2 minutes. In the ideal case, the blood collection was expected to be 20 mL after 2 minutes.[3] However, microbeads have caused resistance in the circuit and the cartridge; as a consequences, the amount of blood in the tests for the CAGO-22% and CAGO-17% beads were found to be only about ~14 mL (7 mL min^{-1}). There may have been two reasons for the lower flow rate: first, the blood was a rather viscous substance than the deionized water (no beads), since the actual flow rate for a control experiment by replacing blood with deionized water was found to be ~18 mL (9 mL min^{-1}). Therefore, it seemed that the higher viscosity of the blood resulted in the greater resistance of the flow and thus lowered the actual flow rate. Secondly, it may have been due to the dimensions of the cartridge as the cartridge was designed to be longer and thinner to ensure that the blood could have a better contact with the adsorbent in a relatively longer residence time. Nevertheless, such dimensions led to a greater resistance of the flow. In addition to the blood flow rate, we have performed a blood loss test in the cartridge as shown on the image in Supporting Figure S5c. The experimental setup was similar to the flow rate test, but the major difference was the blood returned to the beaker instead of the measuring cylinder. The circulation was maintained for 10 minutes for both the CAGO-22% and CAGO-17% to measure the blood loss. For each analysis, the blood was about 60 mL at the beginning and, after the circulation for 10 minutes under the flow rate of 10.01 mL (flow rate of the pump), the remaining amount of blood for the CAGO-22% and CAGO-17% was found to be

about ~52 mL, representing an 87% blood recovery. A portion of the blood was found to retain in the wall of the cartridge, adsorbents, and the junction parts, which accounted for the blood loss after the analysis.[4-5]

b. Blood retention test:

The retention of the blood cells was calculation with following equation:

$$Retention = \frac{Final\ concentration}{Initial\ concentration} \times 100\% \quad (1)$$

Where: $Concentration = average\ \#\ of\ cells\ per\ square \times dilution\ factor \times 10^4$ (2)

In case of only blood cells: The number of blood cells counted are 13, and the concentration of initial blood sample is:

$$\frac{13}{(16\times4)} \times 400 \times 10000 \times 10000 = 8.125 \times 10^9 \text{ cells mL}^{-1}$$

In case of CAGO-22%: The number of blood cells counted are 11, and the concentration of initial blood sample is:

$$\frac{11}{(16\times4)} \times 400 \times 10000 \times 10000 = 6.875 \times 10^9 \text{ cells mL}^{-1}$$

the retention of the blood cells for CAGO-22% is 84.62%

In case of CAGO-17%: The number of blood cells counted are 10, and the concentration of initial blood sample is:

$$\frac{10}{(16\times4)} \times 400 \times 10000 \times 10000 = 6.25 \times 10^9 \text{ cells mL}^{-1}$$

The retention of the blood cells incubated for CAGO-22% is 76.92%

After the calculations, it was found that the initial concentration of blood was $8.125*10^9$ cells mL^{-1}, while the final concentration for CAGO-22% and CAGO-17% was $6.875*10^9$ and $6.25*10^9$ cells mL^{-1}, therefore, the retention for CAGO-22% and CAGO-17% for blood cells after passing through the column was 84.62% and 76.92%.

Calculation for white blood cells (WBC) count: The retention of the white blood cells is as follows:

For WBC as control:

$$\frac{23}{(16x4)} \times 400 \times 10000 \times 10000 = 1.437 \times 10^{9} \text{ cells mL}^{-1}$$

For WBC count for CAGO-22%:

$$\frac{21}{(16x4)} \times 400 \times 10000 \times 10000 = 1.312 \times 10^{9} \text{ cells mL}^{-1}$$

For WBC count for CAGO-17%:

$$\frac{17}{(16x4)} \times 400 \times 10000 \times 10000 = 1.062 \times 10^{9} \text{ cells mL}^{-1}$$

After the calculations, it was found that the initial concentration of WBC was $1.437x10^{9}$ cells mL^{-1}, while the final concentration for CAGO-22% and CAGO-17% was $1.312x10^{9}$ and $1.062x10^{9}$ cells mL^{-1}, therefore, the retention for CAGO-22% and CAGO-17% for blood cells after passing through the column was 91.3% and 73.9%.

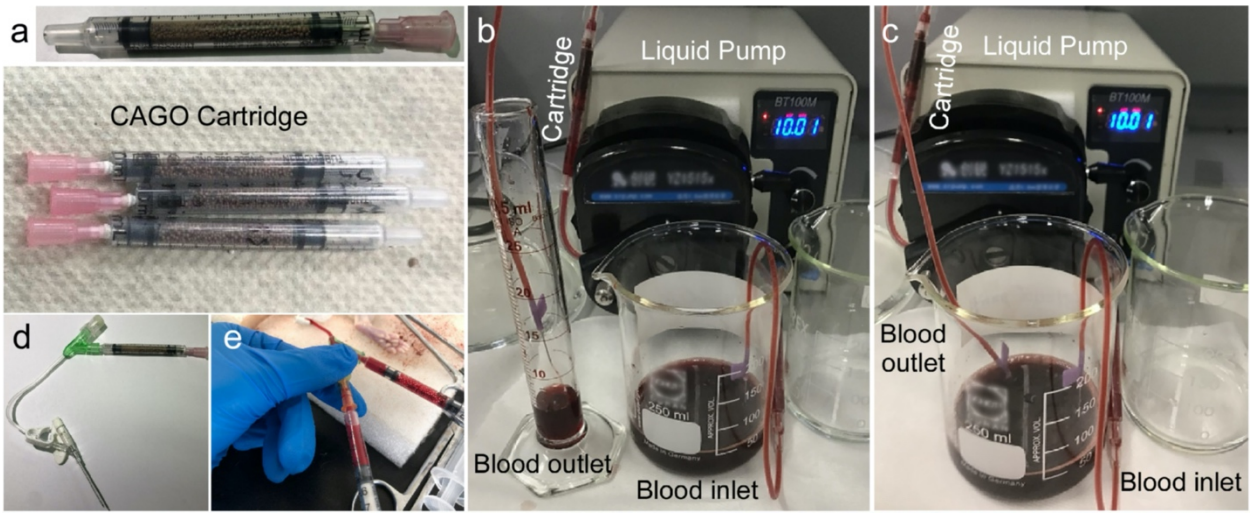

Figure S5. **For *in vivo* analysis for uric acid and creatinine removal arrangements.** (a) The image of a filled cartridge, the dark brown material shown in the cartridge was the adsorbent, it is closely packed inside the cartridge to obtain the better contact with the blood and cartridge for cellulose acetate and graphene oxide, (b) Setup for actual blood flow rate. (c) Setup for actual blood loss. Cartridge in connected loop with the (d) before experiment, and after the experiment (e).

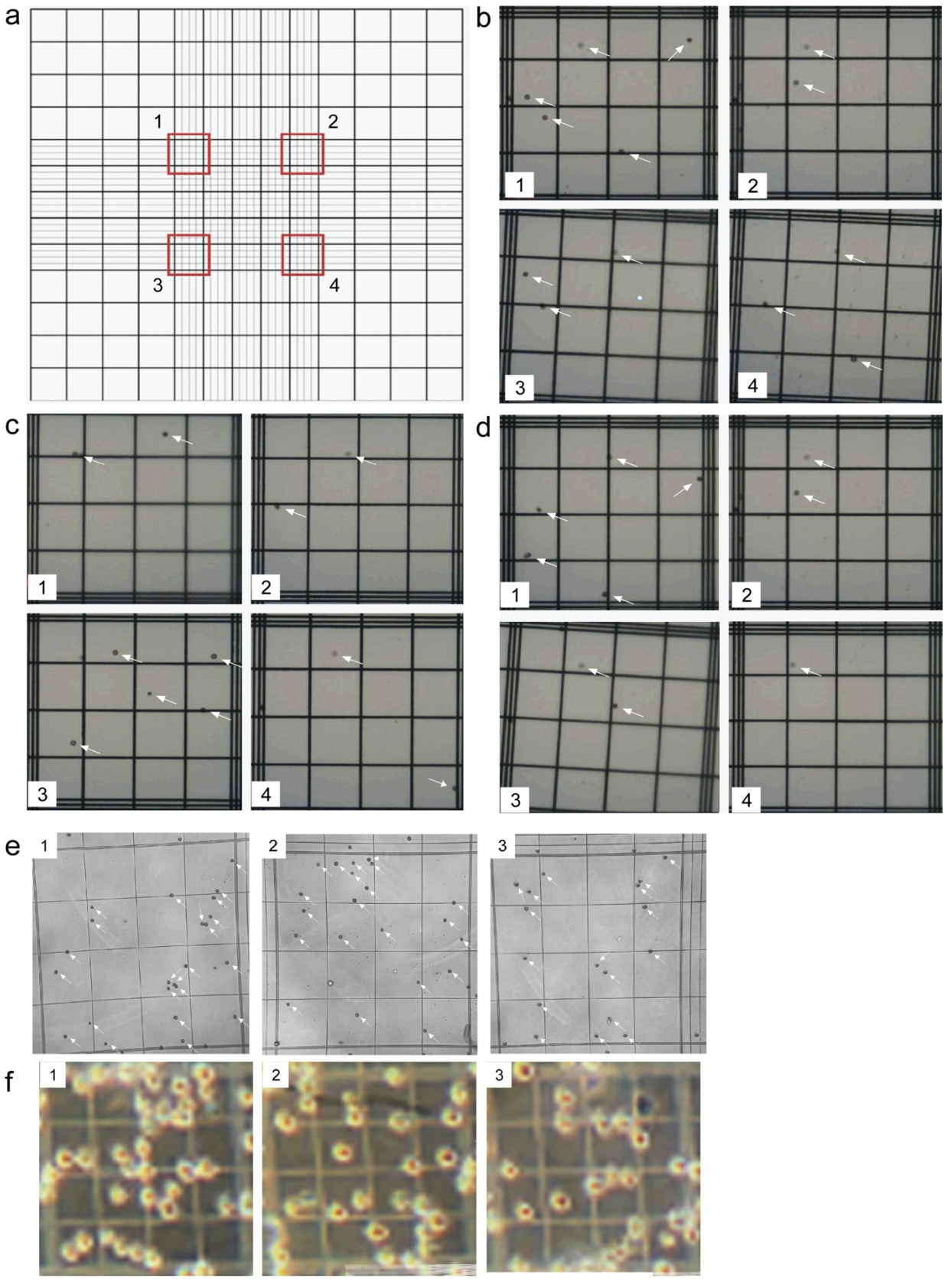
a
1
2
3
4
b
1
2
3
4
c
1
2
3
4
d
1
2
3
4
e
1
2
3
f
1
2
3

Figure S6: The blood retention test using Hemocytometer counting chamber. (a) The layout of Hemocytometer counting chamber, here red square shows the area for imaging of the blood cells counting. (b) The microscopic images showing the blood cells retained for the blood cells as control sample are 13 blood cells, (c) the blood cell counting for CAGO-22%, the number of cells is 11, (d) the blood cell counting for CAGO-17%, the number of cells is 10. Images were taken under microscope 4X (each square with area of 2.5mm×2.5mm). (e) The white blood cell retention test using Hemocytometer counting chamber. (1) The microscopic images showing the white blood cells retained for the blood cells as control sample are 23 white blood cells, (2) the blood cell counting for CAGO-22%, the number of cells is 21, (3) the blood cell counting for CAGO-17%, the number of cells is 17. (f) The platelet count for the blood cells was done, the microscopic image for platelet count is, (1) for control is 25, (2) for CAGO-22% is 20, and (3) for CAGO-17% is 17. Images were taken under microscope (each square with area of 2.5mm×2.5mm).

S No.	Element	Position BE (eV)	Atomic mass	Atomic Conc. %	Mass Conc.%
1	Oxygen	532.80	15.99	34.79	41.22
2	Carbon	287.00	12.01	63.79	56.74

Table S4: X-ray photoelectron spectroscopy (XPS) for graphene oxide. The elemental information obtained for oxygen and carbon.

3. Molecular modeling and simulations:

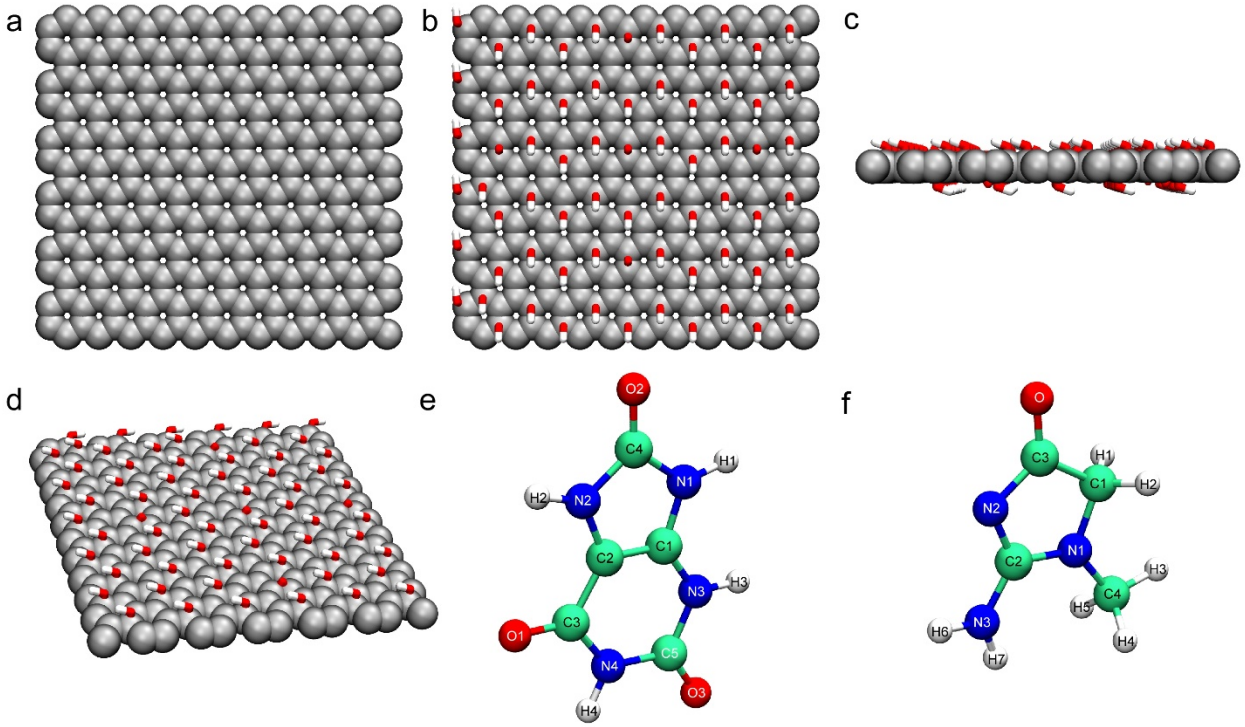

Figure S7. The design for functionalized graphene uric acid and creatinine. (a) The top view of bare graphene sheet, (b) The top view of functionalized graphene with uniformly distributed epoxy, hydroxyl and carboxyl groups, (c) side view of GO sheet, (d) side tilted view of GO sheet, (e) chemical structure of uric acid with naming of atoms, (f) structure of creatinine with the naming of atoms.

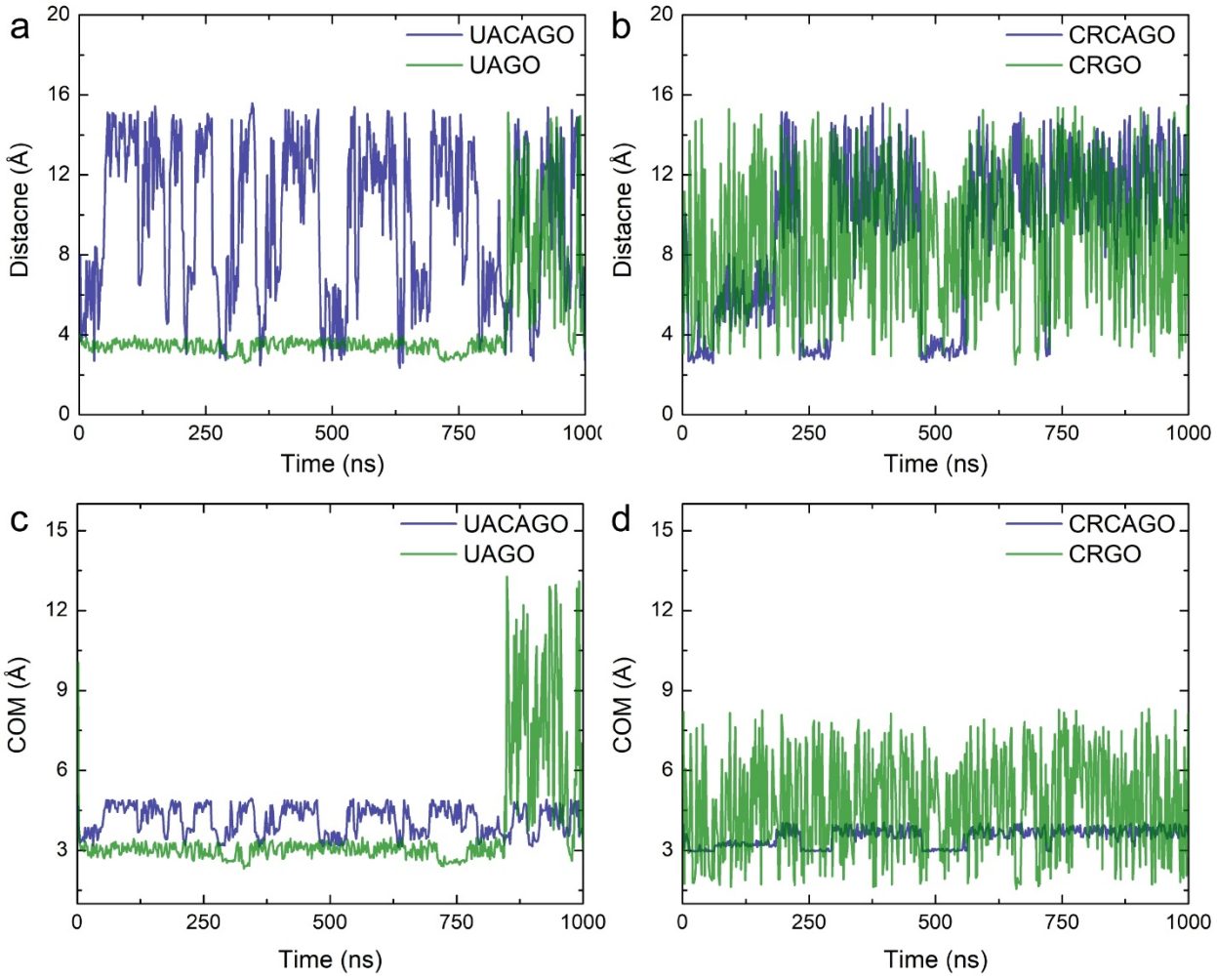

Figure S8: Movement of uric acid and creatinine along z axis. The distance along the z axis for uric acid on GO and GOCA (a) For uric acid, (b) For creatinine. The center of mass (COM) movement on GO and COCA (c) For uric acid, (d) For creatinine.

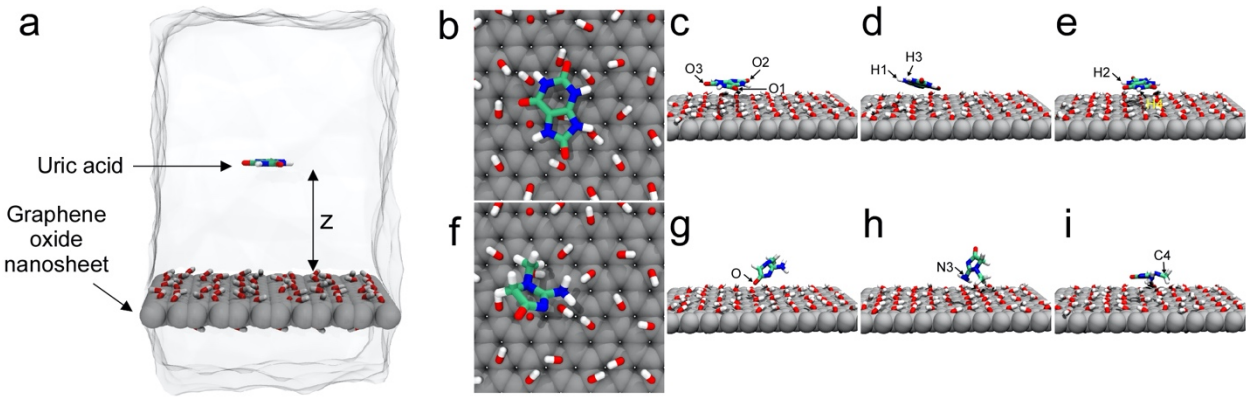

Figure S9. Confirmation for uric acid and creatinine on GO surface. (a) The uric acid was kept at a distance of z = 15 Å above the GO sheet, at which interactions between the molecules and GO become negligible, similar setup was employed for creatinine adsorption. (b) Uric acid adsorption snapshots for the confirmation and orientations. Orientation of atoms in uric acid on GO (c) for oxygen O1, O2, and O3 atoms, (d) for hydrogen atoms H2 and H4, (e) for hydrogens atoms H1 and H3. (f) Creatinine adsorption snapshots for confirmations and orientation for (g) for oxygen atom, (h) for N3 atom with two hydrogen atoms, (i) for C4 atom with three hydrogen atoms.

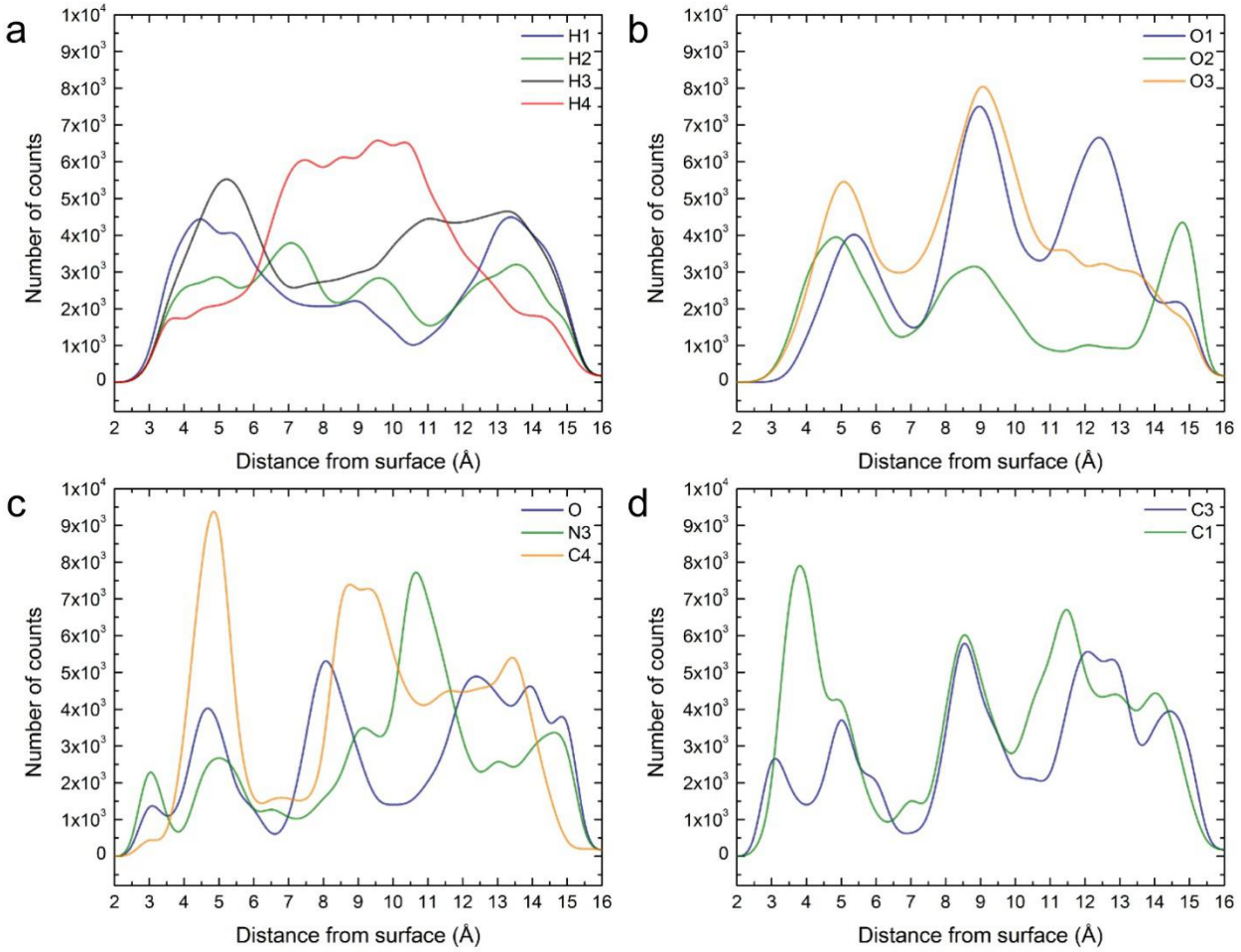

Figure S10: Histogram for uric acid and creatinine on cellulose acetate-graphene oxide. The distance analyzed are for those atoms of hydrogen attached to carbon and nitrogen groups for creatinine molecule. The histogram for uric acid molecule on GOCA surface (a) For hydrogen atoms H1, H2, H3, and H4 atoms, (b) For oxygen atoms O1, O2, and O3. The histogram for creatinine atoms on GOCA surface (c) For oxygen (O), nitrogen (N3), and carbon (C4), d) For carbon atoms (C1 and C3).

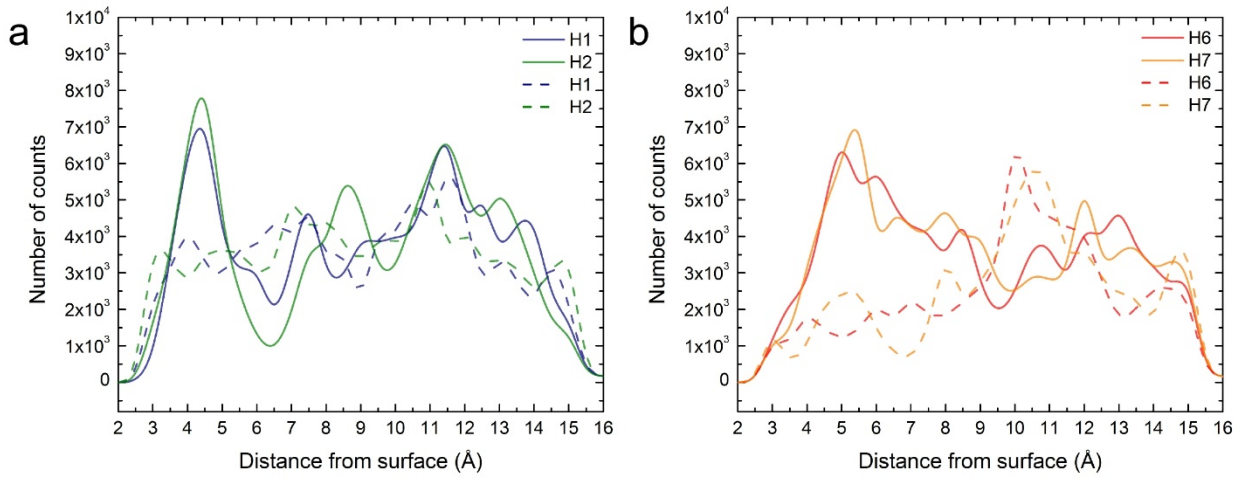

Figure S11: Histogram for uric acid and creatinine on GO and CAGO. The distance analyzed are for those atoms of hydrogen attached to carbon and nitrogen groups for creatinine molecule, the histogram for creatinine atoms with solid line represent on CA-functionalized GO and dash line on GO by MD simulations, (a) For hydrogen atoms (H1 and H2), (b) For hydrogen atoms (H6 and H7).

Reference

(1) Peng, Z.-Y.; Zhang, J.; Rimmelé, T.; Zhou, F.; Chuasuwan, A.; Kaynar, A. M.; Kellum, J. A. Development of Venovenous Extracorporeal Blood Purification Circuits in Rodents for Sepsis. *Journal of Surgical Research* **2013,** *185* (2), 790-796, DOI: 10.1016/j.jss.2013.07.020.
(2) Yorimitsu, D.; Satoh, M.; Koremoto, M.; Haruna, Y.; Nagasu, H.; Kuwabara, A.; Sasaki, T.; Kashihara, N. Establishment of a Blood Purification System for Renal Failure Rats Using Small-Size Dialyzer Membranes. *Therapeutic Apheresis and Dialysis* **2012,** *16* (6), 566-572, DOI: 10.1111/j.1744-9987.2012.01091.x.
(3) Topping, D. L.; Storer, G. B.; Trimble, R. P. Effects of Flow Rate and Insulin on Triacylglycerol Secretion by Perfused Rat Liver. *American Journal of Physiology-Endocrinology and Metabolism* **1988,** *255* (3), E306-E313, DOI: 10.1152/ajpendo.1988.255.3.E306.
(4) Choi, J.; Reipa, V.; Hitchins, V. M.; Goering, P. L.; Malinauskas, R. A. Physicochemical Characterization and In Vitro Hemolysis Evaluation of Silver Nanoparticles. *Toxicological Sciences* **2011,** *123* (1), 133-143, DOI: 10.1093/toxsci/kfr149.
(5) Keong, L. C.; Halim, A. S. In vitro Models in Biocompatibility Assessment for Biomedical-grade Chitosan Derivatives in Wound Management. *Int J Mol Sci* **2009,** *10* (3), 1300-1313, DOI: 10.3390/ijms10031300.